Optimal design of measurement settings for quantum-state-tomography experiments

Jun Li,[1,2,*] Shilin Huang,[3,2,†] Zhihuang Luo,[1,2] Keren Li,[4,2] Dawei Lu,[5,2] and Bei Zeng[6,2,‡]

[1]*Beijing Computational Science Research Center, Beijing 100193, China*

[2]*Institute for Quantum Computing, University of Waterloo, Waterloo N2L 3G1, Ontario, Canada*

[3]*Institute for Interdisciplinary Information Sciences, Tsinghua University, Beijing 100084, China*

[4]*Department of Physics, Tsinghua University, Beijing 100084, China*

[5]*Department of Physics, Southern University of Science and Technology, Shenzhen 518055, China*

[6]*Department of Mathematics and Statistics, University of Guelph, Guelph N1G 2W1, Ontario, Canada*

(Received 17 May 2017; published 6 September 2017)

Quantum state tomography is an indispensable but costly part of many quantum experiments. Typically, it requires measurements to be carried out in a number of different settings on a fixed experimental setup. The collected data are often informationally overcomplete, with the amount of information redundancy depending on the particular set of measurement settings chosen. This raises a question about how one should optimally take data so that the number of measurement settings necessary can be reduced. Here, we cast this problem in terms of integer programming. For a given experimental setup, standard integer-programming algorithms allow us to find the minimum set of readout operations that can realize a target tomographic task. We apply the method to certain basic and practical state-tomographic problems in nuclear-magnetic-resonance experimental systems. The results show that considerably fewer readout operations can be found using our technique than by using the previous greedy search strategy. Therefore, our method could be helpful for simplifying measurement schemes to minimize the experimental effort.

DOI: 10.1103/PhysRevA.96.032307

I. INTRODUCTION

The problem of estimating an unknown quantum state is of fundamental importance in quantum physics [1] and especially in the field of quantum information processing, such as quantum computation [2], quantum cryptography [3], and quantum system identification [4]. Quantum state tomography aims to determine the full state of a quantum system via a series of quantum measurements. It has become an indispensable tool in almost any experimental physical setup. The standard tomography procedure applied for complete reconstruction of a d-dimensional quantum state consists of projecting the density operator with respect to at least $(d^2 - 1)$ measurement operators. A reconstruction based on linear-squares inversion [5] or maximum-likelihood estimation [6] is then used to calculate the best-fit density matrix for the experimentally acquisited data set. Apparently, tomography is not an efficient process and can be extremely computationally costly for even modest-sized systems.

In recent years, state tomography has been an increasingly challenging task as the number of controllable qubits in quantum experiments is steadily growing. With the rapid progress of experimental control techniques, the size of quantum systems with entanglement or coherence prepared in the laboratory has already grown to 8–10 qubits in photonic systems [7–9], 12 qubits in nuclear-magnetic-resonance (NMR) systems [10], and even 14 qubits in ion traps [11]. Needless to say, performing state-estimation tasks on such systems is tedious and time-consuming. Improved techniques for quantum state tomography would certainly impact a wide range of applications in experimental physics. For example, Ref. [12] used hundreds of thousands of measurements and weeks of postprocessing to get a maximum-likelihood estimate of an entangled state of eight trapped-ion qubits. Later, this experiment was simplified as there was put forward a much more economic tomographic scheme, which is based on the concept of mutually unbiased bases and promises to reduce about 95% of the number of measurements required [13]. To give another example, in Ref. [14] it was shown that, in reconstructing a 14-qubit state, using both a smart choice of the state representation and parallel graphic-processing-unit programming can speed up the postprocessing by a factor of 10^4. Besides these technical improvements, there also exist various theoretical approaches that are devoted to enhancing the capability of quantum state tomography [15–17]. Most of them either extract partial information or exploit some prior information about the state to be reconstructed.

In this paper, we are concerned with the design of the measurement scheme in a tomographic experiment. Our study is primarily motivated by a problem which is present in many experimental platforms; namely, state tomography often involves informationally overcomplete measurements. The reason can be stated as follows. Normally, a tomographic experiment consists of a series of different measurement settings, and from each single measurement setting a bunch of data are recorded. Here, a measurement setting refers to a particular configuration of the experimental measurement apparatus. For example, in photonic systems one can tune the wave plates and polarizers to make arbitrary local polarization measurements, so a setting means the choice of one observable per qubit and repeated projective measurements in the observables' eigenbases [18]. In NMR, a measurement setting corresponds to taking a spectrum. Because NMR experiments are performed on a large ensemble of molecules, the expectation values of the observables (not necessarily

*lijunwu@mail.ustc.edu.cn

†eurekash.thu@gmail.com

‡zengb@uoguelph.ca

 ©2017 American Physical Society

compatible) can be read out from a single spectrum [19]. In both platforms, there could be considerable overlap between the experimental outcomes acquired from different measurement settings; that is, there are redundant measurements. Moreover, switching from one measurement setting to another could be time intensive or error prone. Therefore, it is desirable to find out what the minimum number of measurement settings that suffices to determine the state of the system is. A judicious experiment design would certainly help improve the efficiency of tomographic reconstruction. The purpose of this paper is to address this question via integer-programming techniques. In the following, we shall first formulate the problem of optimal tomographic experiment design in terms of integer programming. Then, we concentrate on optimizing the design of a readout pulse set in the context of nuclear magnetic resonance.

II. OPTIMAL EXPERIMENT DESIGN

We restrict our consideration to the case of n qubits; higher-dimensional systems can be treated similarly. An n-qubit system's state is represented by a 2^n-dimensional density matrix denoted as ρ, which is Hermitian and semipositive definite and has unit trace. A convenient and equivalent description of the quantum system is given by the Bloch vector. Let $\{B_k\}_{k=1}^{4^n-1}$ be some orthonormal basis for the space of traceless Hermitian operators satisfying the condition that for any $k,j=1,\ldots,n$, $\mathrm{Tr}(B_kB_j)/2^n=\delta_{kj}$. Then decomposed with respect to this basis, ρ can be viewed as a point $\boldsymbol{r}$ in a (4^n-1)-dimensional real vector space: $\rho=I^{\otimes n}/2^n+\sum_{k=1}^{4^n-1}\boldsymbol{r}_kB_k$, with I being the two-dimensional identity matrix and $\boldsymbol{r}_k=\mathrm{Tr}(\rho B_k)/2^n$. Clearly, full tomography amounts to measuring all of the quantities $\{\mathrm{Tr}(\rho B_1),\ldots,\mathrm{Tr}(\rho B_{4^n-1})\}$.

Experimenters primarily work in two different bases, the computational basis and the product-operator basis. In the computational basis the rows and columns of the density matrix ρ are labeled by the binary expansion of their indices from $|0\cdots0\rangle$ to $|1\cdots1\rangle$. The product-operator basis, defined as $\mathcal{P}_n=\{P_k\}_{k=1}^{4^n-1}=\{I,X,Y,Z\}^{\otimes n}/\{I^{\otimes n}\}$, where X,Y,Z are the three Pauli matrices

$$X=\begin{pmatrix}0&1\\1&0\end{pmatrix},\quad Y=\begin{pmatrix}0&-i\\i&0\end{pmatrix},\quad Z=\begin{pmatrix}1&0\\0&-1\end{pmatrix},$$

is a commonly used tool in describing pulse-control experiments. It provides at the same time physical insight into the experimental setup (e.g., in NMR) and computational convenience [20]. In the following we work on the product-operator basis $\mathcal{P}$, but there is no problem in extending our analysis to other bases.

In performing a tomographic experiment, we send multiple copies of the state ρ to our measurement apparatus. The apparatus can be configured in different settings. Suppose that under a specific measurement setting, we can read out the information for the following set of operators: $\mathcal{O}=\{O_1,\ldots,O_k,\ldots\}$, where $O_k\in\mathcal{P}$. The experimental tomography procedure employs a series of measurement settings, each corresponding to the observation of a different set of operators. Here, the switch between measurement settings is implemented through either changing the configuration of the detectors or adding a unitary readout operation before data acquisition. This can

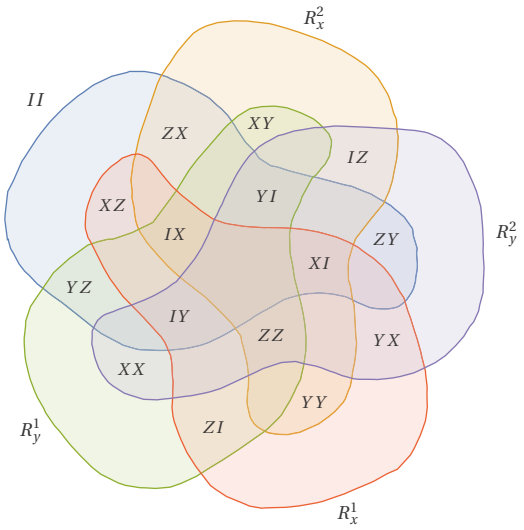

FIG. 1. Venn diagram visualizing the set cover problem for a two-qubit state-tomography task. Here, the readout operations are restricted to the identity operation and single-qubit rotations. This is a very simple instance that occurs when we want to perform state tomography for a homonuclear two-spin system in NMR. Clearly, any and no less than four of the five sets suffice to cover the entire measurement basis.

be readily seen from the equality $\mathrm{Tr}(U\rho U^\dagger E)=\mathrm{Tr}(\rho UEU^\dagger)$, where E is an arbitrary observable and $U\in SU(2^n)$. For instance, in order to measure the three Cartesian components of a spin, if we can observe only two Pauli operators in one experimental setting, we will need two readout operations, which can be selected from the set $\{I,R_x,R_y\}$, where R_x and R_y are the $\pi/2$ rotations about the x and y axes, respectively.

Now suppose we have the following experimentally available set of readout operations: $\mathcal{U}=\{U_1,\ldots,U_j,\ldots\}$. We denote $\mathcal{S}=\{S_1,\ldots,S_j,\ldots\}$, where S_j corresponds to the set of measurement operators generated through U_j: $S_j=\{U_jO_kU_j^\dagger|O_k\in\mathcal{O}\}$. We assume that $S_j\subseteq\mathcal{P}$ for any j. Here, some abuse of notation occurs as, actually, we should ignore the global phase and coefficient. Then $\mathcal{S}$ is a collection of $|\mathcal{U}|$ subsets of $\mathcal{P}$, each containing $|\mathcal{O}|$ elements. Clearly, to ensure full state tomography, a necessary condition is that $\mathcal{P}$ should be covered by $\mathcal{S}$, that is, $\mathcal{P}=\bigcup_j S_j$. Now, we can state the central problem of this work, that is, to identify the smallest subcollection of $\mathcal{S}$ whose union equals $\mathcal{P}$. More formally, we are considering a standard set cover problem, which we denote by $\mathbf{P}(\mathcal{P},\mathcal{O},\mathcal{U})$: given $\mathcal{P}$, $\mathcal{O}$, and $\mathcal{U}$, we want to select a subset of readout operations $\{U_j\}\subseteq\mathcal{U}$ with the number of elements as small as possible and such that $\mathcal{P}$ is covered by the set $\{U_jO_kU_j^\dagger|O_k\in\mathcal{O},\{U_j\}\subseteq\mathcal{U}\}$. Figure 1 shows a simple instance of the problem.

The set cover problem is known to be NP-hard in general, meaning that finding an efficient algorithm that can solve it in a reasonable amount of time is unlikely. It is worthwhile to study heuristics for solving the problem with the goal of obtaining a performance guarantee or approximation guarantee on the heuristic. Practically, greedy strategy is widely used for set cover problems. The greedy algorithm proceeds according to a simple rule: in each step, choose the set S_j containing

the largest number of uncovered elements. The algorithm ends until all elements of $\mathcal{P}$ are covered. Reference [21] exploited this method in designing a readout pulse set in NMR. Note that the greedy algorithm generally does not yield the optimal result. Different choices for the first few readout operations in the iteration yield lists that are slightly longer or shorter than those shown. It is in essence an approximation algorithm, which achieves an approximation ratio of $\Theta(\ln|\mathcal{P}|)$ [22]. It can even be shown that no polynomial-time approximation algorithm can achieve a much better approximation bound [23].

Here, we attempt to find the optimal solution for relatively small sized quantum systems. To this end, we resort to an integer-linear-programming formulation of the set cover problem [24]. Let x denote a $|\mathcal{U}|$-element column vector, in which each element x_j is a zero-one variable. The intention is that $x_j = 1$ iff set S_j is chosen in the optimal solution. Let $f(x) = \sum_j c_j x_j$ denote the cost function, where $c_j > 0$ is the cost corresponding to the choice of S_j. In the case of the minimum set cover problem, the cost function is just $f(x) = \sum_j x_j = \|x\|_1$. Let A be a $[(4^n - 1) \times |\mathcal{U}|]$-dimensional matrix with its entries given by $A_{kj} = 1$ ($k = 1, \ldots, 4^n - 1$) if $P_k \in S_j$ and zero otherwise. Now we have the following zero-one integer-programming problem:

$$\begin{aligned} \min \quad & \|x\|_1, \\ \text{subject to} \quad & Ax \geqslant 1, \\ & x_j \in \{0,1\}. \end{aligned}$$

There are a variety of algorithms that can be used to solve integer linear programs exactly, which we do not intend to expand here. Interested readers are referred to [25,26] for the basics. For now, we make several comments:

(1) *Choosing readout operations*. For a quantum system that allows for universal control, the readout operation U can be chosen from the Clifford group $\mathcal{C}$. This is because the Clifford group is the normalizer of the Pauli group [27]; that is, for any U, a Clifford operation, and O, a Pauli observable, if we ignore the global phase and coefficient, $UOU^\dagger$ gives again a Pauli observable. However, the size of the Clifford group is $|\mathcal{C}(n)| = 8\prod_{k=1}^{n} 2(4^k - 1)4^k$, which makes the corresponding integer-programming problem quickly become too huge to handle. Therefore, it is difficult to consider the entire Clifford group in the integer-programming approach. More realistically, we would restrict the problem to just local operations. But notice that in many practical cases the set of single -qubit rotations is not sufficient for covering the whole measurement basis, and then local Clifford operations should be considered.

(2) *Cost function*. Integer programming allows us to consider different cost functions. In practice, more often than not, technical constraints permit only a nonideal set of measurements. For example, the qubits can be individually addressed, whereas nonlocal quantities cannot be measured directly. It is also very common that nonlocal operations are less accurate than local operations. In such cases, we would prefer to choose local operations, and this can be achieved simply through assigning low costs to these preferred operations.

(3) *Symmetry consideration*. Many practical tomographic instances contain a great deal of symmetry. One direct consequence is that the optimal solution is not unique. A very useful technique that allows a substantial reduction of the amount of computation required in running integer-programming algorithms is to exploit the symmetry of the problem considered [26,28]. It is desirable to use professional software (e.g., [29]) to run integer-programming algorithms as it already takes into account the symmetry issue and so can behave much faster.

III. NMR TOMOGRAPHY

We first briefly describe the basics of state-tomography experiments in NMR [30]. We consider weakly coupled liquid-state NMR systems. An NMR sample is placed in a strong static magnetic field. The direction of the static field is, by convention, defined as the z axis. The system Hamiltonian takes the following form:

$$H = \sum_{k=1}^{n} \Omega_k Z_k/2 + \pi \sum_{k<j}^{n} J_{kj} Z_k Z_j/2, \tag{1}$$

where Ω_k is the precession frequency of the kth spin under the static field and J_{kj} is the coupling between the kth and jth spins. In a NMR experiment, the sample is wound with a detection coil. The precessing magnetization of the sample is detected by the coil and constitutes the free-induction decay (FID). The induced signal is the sum of a number of oscillating waves of different frequencies, amplitudes, and phases. In the spectrometer, this is recorded using two orthogonal detection channels along the x and y axes, known as quadrature detection. The FID is then subjected to Fourier transformation, and the resulting spectral lines are fit, yielding a set of measurement data.

More precisely, let ρ denote the state at the start of the sampling stage; then the measured time-domain signal $F(t)$ resulting from the rotating bulk magnetization is essentially a pair of ensemble averages:

$$\begin{aligned} F(t) &= \mathrm{Tr}\left[e^{-iHt}\rho e^{iHt}\sum_m (X_m + iY_m)\right] \\ &= \mathrm{Tr}\left[\rho e^{iHt}\sum_m (X_m + iY_m)e^{-iHt}\right]. \end{aligned} \tag{2}$$

From this expression, the record of the FID signal $F(t)$ can be thought of as the one in which the measured operators are $\mathcal{O} = e^{iHt}\sum_k (X_k + iY_k)e^{-iHt}$, which can be calculated easily when the Hamiltonian H is specified. Because H is composed of Z and ZZ terms, the measurement operator set $\mathcal{O}$ consists of only single-quantum coherence operators. When measuring other operators is desired, readout pulses should be appended to the experiment.

Now, we give several examples showing how our method developed in the previous section applies to NMR state tomography.

(1) *Tomography via a single probe qubit*. In certain circumstances, we can do better than the numerical optimization: we can write down an analytic expression for an optimal readout scheme. Here, we develop a provably optimal scheme, where we intend to perform tomography via just a single probe qubit.

Of course, to make the scheme work, two conditions must be assumed in advance: (i) the probe qubit is coupled to each of the other $n-1$ qubits; (ii) the multiplets corresponding to the probe qubit can be well resolved. As we have described, the set of measurement operators is just single-quantum coherences, so we have

$$\mathcal{O} = \{X,Y\} \otimes \{I,Z\}^{\otimes n-1}.$$

As such, we would transfer the information of the other qubits to the probe qubit before detection. Let W_{kj} denote the SWAP operation between qubits k and j. Our candidate readout operations are

$$\mathcal{U} = \{VW_{1j} : V \in \{I,R_x,R_y\}^{\otimes n}; j = 1,\ldots,n\}. \quad (3)$$

Let f_n denote the number of experiments used. Now we show that the lower bound for the number of experiments necessary to construct the density operator is as follows.

Proposition 1. $f_n^* = (3^n+1)/2$.

Proof. The correctness of the formula when $n = 1$ is trivial. For $n > 1$, the idea of the proof is to find a recursive relation.

First, we show that $(3^n+1)/2$ is a lower bound. Notice that any $U \in \mathcal{U}$ cannot change the weight of any Pauli element. So each experiment gives only observation results of two weight-n Pauli elements. Since there are 3^n weight-n Pauli elements in $\mathcal{P}$, at least $(3^n+1)/2$ readout operations are needed.

Now we show that this lower bound can be achieved. We provide a constructive way to find an optimal solution. Divide $\mathcal{P}$ into two parts: $\mathcal{P} = \mathcal{P}^{(1)} \cup \mathcal{P}^{(2)}$, where

$$\mathcal{P}^{(1)} = \{X,Y\} \otimes \{I,X,Y,Z\}^{\otimes(n-1)},$$
$$\mathcal{P}^{(2)} = \{I,Z\} \otimes \{I,X,Y,Z\}^{\otimes(n-1)}.$$

To cover $\mathcal{P}^{(1)}$, we select readout operations from

$$\mathcal{U}^{(1)} = I \otimes \{I,R_x,R_y\}^{\otimes(n-1)};$$

to cover $\mathcal{P}^{(2)}$, we select readout operations from

$$\mathcal{U}^{(2)} = \{VW_{1j} : V \in \{I,R_x,R_y\}^{\otimes n}; j = 2,\ldots,n\}.$$

As $\mathcal{U}^1$ and $\mathcal{U}^2$ have no intersections, we get two separate subproblems.

The subproblem $\mathbf{P}(\mathcal{P}^{(1)},\mathcal{O},\mathcal{U}^{(1)})$ is equivalent to the problem $\mathbf{P}(\{I,X,Y,Z\}^{\otimes(n-1)},\{I,Z\}^{\otimes n-1},\{I,X,Y\}^{\otimes(n-1)})$. Since there are $3^{(n-1)}$ weight-$(n-1)$ Pauli elements and each experiment can measure only one of them, we need $3^{(n-1)}$ experiments.

The subproblem $\mathbf{P}(\mathcal{P}^{(2)},\mathcal{O},\mathcal{U}^{(2)})$ can be reduced to

$$\mathbf{P}(\{I,Z\} \otimes \{I,X,Y,Z\}^{\otimes(n-1)},$$
$$\{I,Z\} \otimes \{X,Y\} \otimes \{I,Z\}^{\otimes n-2},$$
$$I \otimes \{VW_{2j} : V \in \{I,R_x,R_y\}^{\otimes n-1}; j = 2,\ldots,n\}).$$

That is, any solution to the latter problem can be mapped to a solution to the former by simply changing the probe qubit from 2 to 1. Note that the latter problem is essentially $\mathbf{P}(\mathcal{P}(n-1),\mathcal{O}(n-1),\mathcal{U}(n-1))$. Therefore, our construction has a recursive relation: $f_n = f_{n-1} + 3^{n-1}$. Starting with $f_1^* = 2$, we then get $f_n = (3^n+1)/2$. Together with the bound analysis at the beginning, we conclude that the lower bound $(3^n+1)/2$ is exact.

Example 1. Iodotrifluroethylene (C_2F_3I) dissolved in D-chloroform was used as a quantum information processor in Refs. [31,32]. The sample's molecular structure is

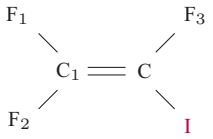

Here, the ^{13}C (C_1) nucleus and the three ^{19}F nuclei (F_1, F_2, and F_3) constitute a four-qubit system. For this molecule, only C_1 can be adequately observed. Therefore, to observe those operators that are relevant to the state of the fluorine nuclei it is necessary to swap the state between them and the carbon before observation. So readout operations can be chosen from the set in Eq. (3). According to our proposition, the minimum number of readout experiments is 41.

(2) Now we consider homonuclear systems, assuming that all peaks on the spectrum can be adequately resolved and observed. In homonuclear systems, all the multiplets are experimentally observed on the same spectrometer channel, so one readout operation, namely, one spectrum, contains n well-resolved multiplets and yields $n2^n$ expansion coefficients. In such an ideal case, we can observe all the single-quantum transition operators from the experimental spectrum. In other words, we will have the following collection of Pauli measurements that can be accessed in a single experiment:

$$\mathcal{O} = \bigcup_{m=1}^{n} (\{I,Z\}^{\otimes(m-1)} \otimes \{X_m,Y_m\} \otimes \{I,Z\}^{\otimes n-m}).$$

One can choose the following readout operation set:

$$\mathcal{U} = \{I,R_x,R_y\}^{\otimes n}.$$

Reference [21] referred to $\mathcal{U}$ as the canonical tomographic pulse set and employed a greedy algorithm to search for a smaller readout pulse set. It turns out that, unlike in the previous example, it is hard to analytically construct an optimal scheme for the current problem. Here, we resort to integer programming. Figure 2 shows our running results, which are listed together with the methods of canonical tomography and greedy search. From Fig. 2, we can see that for a six-qubit system, using the measurement scheme found by integer programming would save around 20% of the experiment time compared with using the greedy method. Moreover, integer programming allows us to confirm that the obtained solution is indeed optimal for a system size up to 5 (see Table I). These results clearly demonstrate the usefulness of the integer-programming technique because we are able to get appreciable improvements over what was obtained before.

IV. SUMMARY

Quantum state tomography plays an essential role in many quantum-information-processing experiments. Developing techniques that allow simplification of state-tomography experiments is particularly pressing in regard to the situation that ever-larger quantum devices are emerging in laboratories. Studies are often concerned with optimizing

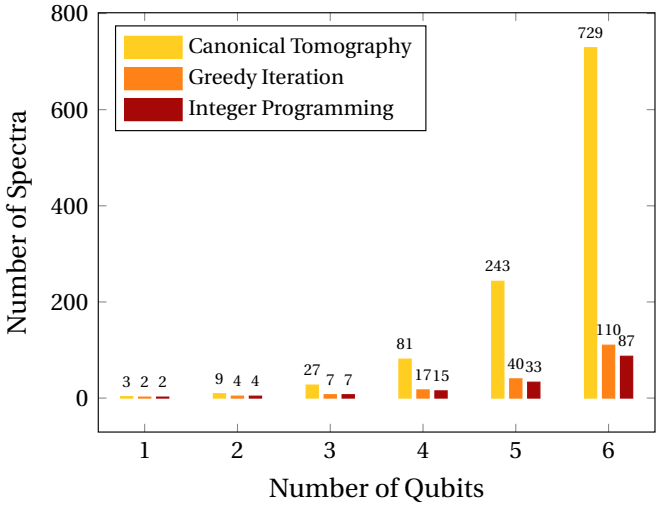

FIG. 2. Comparison of canonical tomography, the results of the iterative greedy algorithm in Ref. [21], and the results of the integer-programming approach for complete tomography on homonuclear n-qubit systems with n between 1 and 6.

the number of required measurements, e.g., measurement schemes that are based on symmetric informationally complete positive operator-valued measures [33]. A bit differently, the problem that we addressed in this work is to reduce the number of required measurement settings. This problem arises when we want to implement a tomographic scheme in a concrete experimental setup. We studied the application of integer programming in solving the problem. The presented test examples confirmed the usefulness of the integer-programming approach. Our method can be easily incorporated into other existing tomographic strategies [34–36]. Also, it is straightforward to generalize our results to various quantum-process-tomography experiments [37,38]. It is our hope that the integer-programming formulation, as developed in this work, will become a useful tool in future tomographic experiments for increasingly large quantum systems, overcoming the roadblock against further development in quantum technologies.

TABLE I. Examples of the optimal pulse set that yields complete tomography on n-spin homonuclear systems for n between 1 and 5.

n	f_n^*	Solution instance
1	2	I, R_x
2	4	II, R_x^2, R_y^2, $R_x^1 R_x^2$
3	7	III, R_y^3, R_y^1, $R_y^2 R_y^3$, $R_x^1 R_y^2 R_x^3$, $R_x^1 R_x^2 R_y^3$, $R_x^1 R_x^2 R_x^3$
4	15	$IIII$, R_x^4, $R_x^1 R_x^4$, $R_x^1 R_y^4$, $R_y^1 R_y^2$, $R_x^2 R_y^3 R_y^4$, $R_y^2 R_x^3 R_y^4$, $R_y^2 R_y^3 R_y^4$, $R_x^1 R_x^2 R_x^3$, $R_x^1 R_y^2 R_y^3$, $R_y^1 R_x^3 R_x^4$, $R_y^1 R_y^2 R_y^3$, $R_x^1 R_x^2 R_x^3 R_x^4$, $R_y^1 R_x^2 R_x^3 R_x^4$, $R_y^1 R_x^2 R_y^3 R_y^4$
5	33	$IIIII$, R_x^5, $R_x^4 R_y^5$, $R_y^4 R_y^5$, $R_x^3 R_y^5$, $R_y^3 R_y^5$, $R_x^2 R_x^3 R_x^4$, $R_y^2 R_y^3 R_y^4$, $R_x^1 R_y^3 R_x^4$, $R_x^1 R_x^2 R_y^4$, $R_x^1 R_y^2 R_y^5$, $R_x^1 R_y^2 R_x^3$, $R_y^1 R_x^3 R_y^4$, $R_y^1 R_y^3 R_y^5$, $R_y^1 R_x^2 R_x^5$, $R_y^1 R_x^2 R_y^3$, $R_y^1 R_y^2 R_y^5$, $R_y^1 R_y^2 R_x^4$, $R_x^2 R_x^3 R_x^4 R_x^5$, $R_y^2 R_y^3 R_x^4 R_x^5$, $R_y^2 R_y^3 R_y^4 R_x^5$, $R_x^1 R_y^3 R_x^4 R_x^5$, $R_x^1 R_x^2 R_y^4 R_x^5$, $R_x^1 R_y^2 R_x^3 R_x^5$, $R_y^1 R_x^3 R_y^4 R_x^5$, $R_y^1 R_x^2 R_x^3 R_x^5$, $R_y^1 R_y^2 R_x^4 R_x^5$, $R_x^1 R_x^2 R_x^3 R_x^4 R_x^5$, $R_x^1 R_x^2 R_x^3 R_y^4 R_y^5$, $R_x^1 R_x^2 R_y^3 R_x^4 R_y^5$, $R_x^1 R_x^2 R_y^3 R_y^4 R_y^5$, $R_y^1 R_y^2 R_x^3 R_x^4 R_y^5$, $R_y^1 R_y^2 R_x^3 R_y^4 R_y^5$

ACKNOWLEDGMENTS

J.L. is supported by the National Basic Research Program of China (Grants No. 2014CB921403, No. 2016YFA0301201, No. 2014CB848700 and No. 2013CB921800), National Natural Science Foundation of China (Grants No. 11421063, No. 11534002, No. 11375167 and No. 11605005), the National Science Fund for Distinguished Young Scholars (Grant No. 11425523), and NSAF (Grant No. U1530401). B.Z. is supported by NSERC and CIFAR.

[1] *Quantum State Estimation*, edited by M. Paris and J. Řeháček, Lecture Notes in Physics Vol. 649 (Springer, Berlin, 2004).

[2] M. A. Nielsen and I. L. Chuang, *Quantum Computation and Quantum Information* (Cambridge University Press, Cambridge, 2000).

[3] N. Gisin, G. Ribordy, W. Tittel, and H. Zbinden, Quantum cryptography, Rev. Mod. Phys. **74**, 145 (2002).

[4] D. Burgarth and K. Yuasa, Quantum System Identification, Phys. Rev. Lett. **108**, 080502 (2012).

[5] T. Opatrný, D.-G. Welsch, and W. Vogel, Least-squares inversion for density-matrix reconstruction, Phys. Rev. A **56**, 1788 (1997).

[6] Y. S. Teo, H. Zhu, B.-G. Englert, J. Řeháček, and Z. Hradil, Quantum-State Reconstruction by Maximizing Likelihood and Entropy, Phys. Rev. Lett. **107**, 020404 (2011).

[7] Y.-F. Huang, B.-H. Liu, L. Peng, Y.-H. Li, L. Li, C.-F. Li, and G.-C. Guo, Experimental generation of an eight-photon Greenberger-Horne-Zeilinger state, Nat. Commun. **2**, 546 (2011).

[8] X.-C. Yao, T.-X. Wang, P. Xu, H. Lu, G.-S. Pan, X.-H. Bao, C.-Z. Peng, C.-Y. Lu, Y.-A. Chen, and J.-W. Pan, Observation of eight-photon entanglement, Nat. Photonics **6**, 225 (2012).

[9] W.-B. Gao, C.-Y. Lu, X.-C. Yao, P. Xu, O. Gühne, A. Goebel, Y.-A. Chen, C.-Z. Peng, Z.-B. Chen, and J.-W. Pan, Experimental demonstration of a hyper-entangled ten-qubit Schrödinger cat state, Nat. Phys. **6**, 331 (2010).

[10] C. Negrevergne, T. S. Mahesh, C. A. Ryan, M. Ditty, F. Cyr-Racine, W. Power, N. Boulant, T. Havel, D. G. Cory, and R. Laflamme, Benchmarking Quantum Control Methods on a 12-Qubit System, Phys. Rev. Lett. **96**, 170501 (2006).

[11] T. Monz, P. Schindler, J. T. Barreiro, M. Chwalla, D. Nigg, W. A. Coish, M. Harlander, W. Hänsel, M. Hennrich, and R. Blatt, 14-Qubit Entanglement: Creation and Coherence, Phys. Rev. Lett. **106**, 130506 (2011).

[12] H. Häffner, W. Hänsel, C. F. Roos, J. Benhelm, D. Chek-al-kar, M. Chwalla, T. Körber, U. D. Rapol, M. Riebe, P. O. Schmidt, C. Becher, O. Gühne, W. Dür, and R. Blatt, Scalable multiparticle entanglement of trapped ions, Nature (London) **438**, 643 (2005).

[13] A. B. Klimov, C. Muñoz, A. Fernández, and C. Saavedra, Optimal quantum-state reconstruction for cold trapped ions, Phys. Rev. A **77**, 060303(R) (2008).

[14] Z. Hou, H.-S. Zhong, Y. Tian, D. Dong, B. Qi, L. Li, Y. Wang, F. Nori, G.-Y. Xiang, C.-F. Li, and G.-C. Guo, Full reconstruction of a 14-qubit state within four hours, New J. Phys. **18**, 083036 (2016).

[15] M. Cramer, M. B. Plenio, S. T. Flammia, R. Somma, D. Gross, S. D. Bartlett, O. Landon-Cardinal, D. Poulin, and Y.-K. Liu, Efficient quantum state tomography, Nat. Commun. **1**, 149 (2010).

[16] D. Gross, Y.-K. Liu, S. T. Flammia, S. Becker, and J. Eisert, Quantum State Tomography via Compressed Sensing, Phys. Rev. Lett. **105**, 150401 (2010).

[17] G. Tóth, W. Wieczorek, D. Gross, R. Krischek, C. Schwemmer, and H. Weinfurter, Permutationally Invariant Quantum Tomography, Phys. Rev. Lett. **105**, 250403 (2010).

[18] J. B. Altepeter, E. R. Jeffrey, and P. G. Kwiat, Photonic state tomography, Adv. At. Mol. Opt. Phys. **52**, 105 (2005).

[19] L. M. K. Vandersypen and I. L. Chuang, NMR techniques for quantum control and computation, Rev. Mod. Phys. **76**, 1037 (2005).

[20] O. W. Sørensen. G. W. Eich, M. H. Levitt, G. Bodenhausen, and R. R. Ernst, Product operator formalism for the description of NMR pulse experiments, Prog. Nucl. Magn. Reson. Spectrosc. **16**, 163 (1984).

[21] G. M. Leskowitz and L. J. Mueller, State interrogation in nuclear magnetic resonance quantum-information processing, Phys. Rev. A **69**, 052302 (2004).

[22] M. T. Goodrich and R. Tamassia, *Algorithm Design and Applications* (Wiley, Hoboken, NJ, 2015).

[23] U. Feige, A threshold of $\ln n$ for approximating set cover, J. ACM **45**, 634 (1998).

[24] V. V. Vazirani, *Approximation Algorithms* (Springer, Berlin, 2004).

[25] D.-S. Chen, R. G. Batson, and Y. Dang, *Applied Integer Programming: Modeling and Solution* (Wiley, Hoboken, NJ, 2009).

[26] F. Margot, Symmetry in integer linear programming, in *50 Years of Integer Programming 1958–2008: From the Early Years to the State-of-the-Art*, edited by M. Jünger, T. Liebling, D. Naddef, G. Nemhauser, W. Pulleyblank, G. Reinelt, G. Rinaldi, and L. Wolsey (Springer, Berlin, 2010), pp. 647–686.

[27] D. Gottesman, Stabilizer codes and quantum error correction, Ph.D. thesis, California Institute of Technology, 1997.

[28] J. Ostrowski, *Symmetry in Integer Programming* (Proquest, Umi Dissertation Publishing, 2011).

[29] Gurobi Optimization, Inc., Gurobi Optimizer Reference Manual, 2016, http://www.gurobi.com.

[30] J.-S. Lee, The quantum state tomography on an NMR system, Phys. Lett. A **305**, 349 (2002).

[31] Z. Luo, C. Lei, J. Li, X. Nie, Z. Li, X. Peng, and J. Du, Experimental observation of topological transitions in interacting multispin systems, Phys. Rev. A **93**, 052116 (2016).

[32] J. Li, R. Fan, H. Wang, B. Ye, B. Zeng, H. Zhai, X. Peng, and J. Du, Measuring Out-of-Time-Order Correlators on a Nuclear Magnetic Resonance Quantum Simulator, Phys. Rev. X **7**, 031011 (2017).

[33] C. M. Caves, C. A. Fuchs, and R. Schack, Unknown quantum states: The quantum de finetti representation, J. Math. Phys. **43**, 4537 (2002).

[34] T. B. Jackson, Quantum tomography with Pauli operators, M.S. thesis, University of Guelph, 2013.

[35] X. Ma, T. Jackson, H. Zhou, J. Chen, D. Lu, M. D. Mazurek, K. A. G. Fisher, X. Peng, D. Kribs, K. J. Resch, Z. Ji, B. Zeng, and R. Laflamme, Pure-state tomography with the expectation value of Pauli operators, Phys. Rev. A **93**, 032140 (2016).

[36] J. Nunn, B. J. Smith, G. Puentes, I. A. Walmsley, and J. S. Lundeen, Optimal experiment design for quantum state tomography: Fair, precise, and minimal tomography, Phys. Rev. A **81**, 042109 (2010).

[37] G. M. D'Ariano and P. L. Presti, Quantum Tomography for Measuring Experimentally the Matrix Elements of an Arbitrary Quantum Operation, Phys. Rev. Lett. **86**, 4195 (2001).

[38] M. Mohseni and D. A. Lidar, Direct Characterization of Quantum Dynamics, Phys. Rev. Lett. **97**, 170501 (2006).